Impact of rimed and unrimed snow on snowfall retrievals at X, Ka, and W band

M. T. Falconi[1], A. von Lerber[2], D. Ori[3], F. S. Marzano[1], and D. Moisseev[2,4]

[1]*Department of Information Engineering, Sapienza University of Rome, Italy and CETEMPS, L'Aquila, Italy*
[2]*Radar Science, Finnish Meteorological Institute, Finland*
[3]*Institute for Geophysics and Meteorology, University of Cologne, Cologne,*
[4]*Department of Physics, University of Helsinki, Finland*
(Dated: 22 June 2018)

Marta Tecla Falconi

1 Introduction

The correlation between the snowfall rate S and the radar equivalent reflectivity factor Ze is challenging due to their dependence on the microphysical properties of snowfall. The variability of the Ze-S and S-Ze relations at millimeter and centimeter wavelengths is largely affected by microphysical snow growth processes. When a Ze-S power-law relation is assumed, its coefficients depend on different parameters such as the snow type, degree of riming and aggregation, density and terminal velocity (e.g., Von Lerber et al., 2017). The Ze-S relation is also strongly dependent on radar frequency since various electromagnetic wavelengths are more sensitive to different parts of the particle size distribution (PSD).

The radar-based snowfall intensity retrieval at X, Ka and W band has been investigated in previous works (e.g., Falconi et al., 2018) in terms of Ze-S relation using data from four snowfall events, recorded during the Biogenic Aerosols Effects on Clouds and Climate (BAECC) campaign in Finland. The dataset was divided in rimed and unrimed snow using the liquid water path (LWP) as an indicator of riming occurrence and as the driven observable for the k-means clustering of the dataset. This classification highlighted three different regimes: lightly rimed (LR), moderately rimed (MR) and heavy rimed (HR) snow on temporal scales larger than few minutes.

In this work, the four case studies of the 2014 winter from BAECC are used to illustrate the impact of the rimed snow classification for every different instrument available and illustrated in Figure 1.

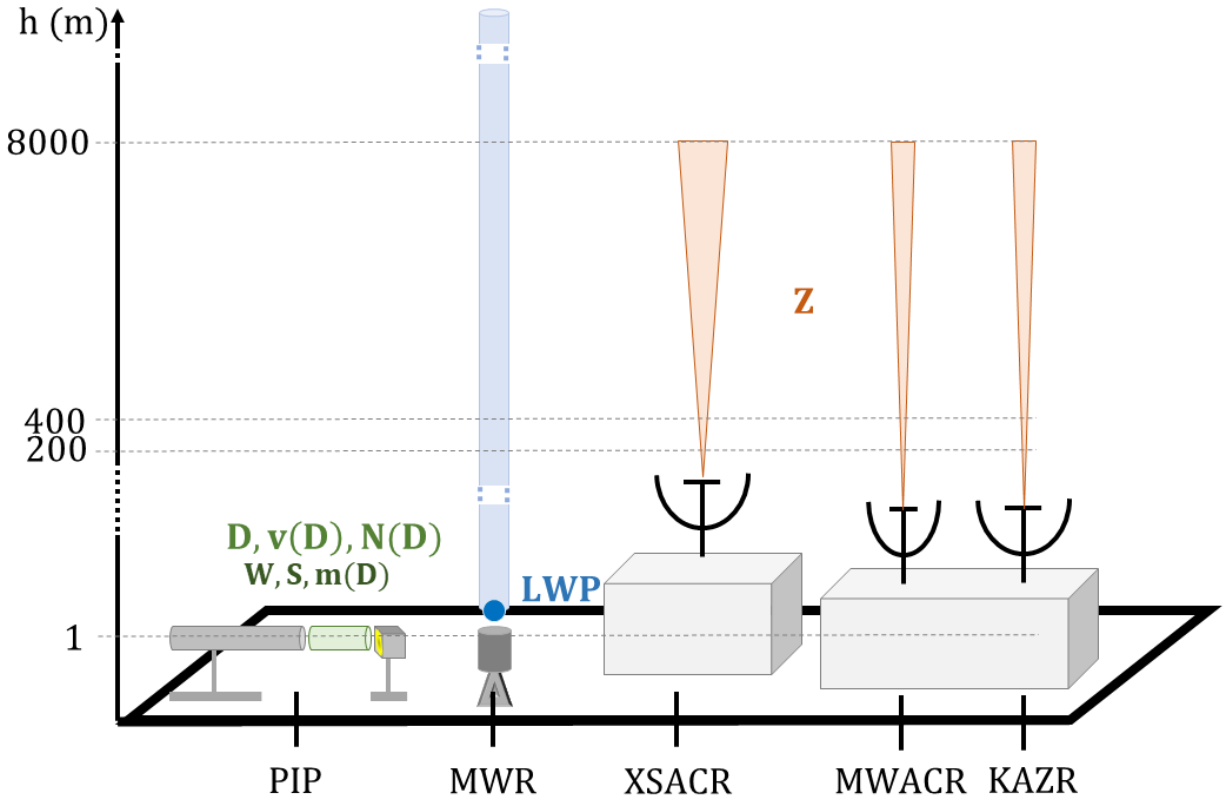

Figure 1:Graphical representation of the measurement site with in situ, video disdrometer (PIP), and remote sensing instruments, microwave radiometer (MWR) and X, Ka and W band radar (XSACR, KAZR, MWACR), deployed during the BAECC campaign.

2 Data, Instruments and Methods

The data used in this study are part of the BAECC campaign organized in 2014 by the University of Helsinki (UH), the US department of Energy ARM program, the Finnish Meteorological Institute (FMI) and other collaborators. The four case studies (12 February, 15-16 February, 21-22 February and 20 March 2014) belong to the snowfall intensive observation period (BAECC SNEX IOP) carried out thanks to a collaboration with the NASA Global Precipitation Measurement (GPM) ground validation program. Figure 1 illustrates the instruments of the BAECC SNEX IOP used in this study. For further information on the single instruments and calibration techniques applied see Falconi et al., 2018.

The focus of this study is to investigate how the impact of the rimed snow classification, made with the microwave radiometer, appears using other instruments.

2.1 Ground-based and microwave radiometer measurements

The rimed snow classification, considered as a reference for this study, was applied in Von Lerber et al., 2017 and Falconi et al., 2018 using the LWP as a proxy of riming. The LWP (gm^{-2}) is an integrated measurements derived from the second Mobile Facility (AMF2) two-channel microwave radiometer (MWR) following the well-known formula:

$$LWP = \int_{h=0}^{\infty} W(h)dh \qquad (2.1)$$

where the W is the liquid water content (in gm^{-3}) and h is the measured height (in m).

As a first proof of this classification we want to use derived variables from the video disdrometer (Particle Imaging Package, PIP). The PIP measures hydrometeor size, fall velocity, an estimate of particle shape and PSD. The liquid water content W and the liquid-water-equivalent snowfall rate S (in mm to hours) are the two variables, evaluated from PIP, used to test the rimed snow classification with in-situ measurements. The W is derived from the third-moment M_3 of the PSD as:

$$W = \frac{\pi}{6}\rho_w 10^{-3} M_3 \qquad (2.2)$$

where ρ_w is the liquid water density (in gcm^{-3}). The S is derived from the mass-flux as

$$S(mmh^{-1}) = 3.6 \int \frac{m(D)}{\rho_w(D)} v(D)\, N(D) dD \qquad (2.3)$$

where D is the particle diameter (in mm), m is the mass (in g) derived as in Von Lerber et al., 2017, v is the velocity (in ms^{-1}) and N is the PSD (in $\mathrm{mm}^{-3}\mathrm{m}^{-1}$). We will use the S(W) to separate the three classes: LR, MR and HR.

2.2 Supervised Classification using radars at X, Ka and W band

The Atmospheric Radiation Measurement (ARM) cloud radars at X, Ka and W band are an important part of the BAECC SNEX IOP. To compare the radars with the ground-based sensors, and also to reduce the beam mismatch, all the data are averaged to 5 min. The near-field influence is also taken into account by selecting all radar data at 400 m (Sekelsky, 2002), as highlighted in Figure 1.

Supervised Maximum Likelihood Classification (MLC) has been used for analysis of rimed classes. The equivalent reflectivity factor Z_e in dBZ, measured by the radar systems at different wavelengths has been divided in three classes (LR, MR, and HR) for each band. The 3x3 matrix of radar measurements is then used to obtain the related probability distribution function (PDF).

The MLC is applied with the arg-max criterion:

$$\hat{c} = \underset{c=LR,MR,HR}{argmax}\ L(Z) \qquad (2.4)$$

where c are the three rimed classes and $\hat{c}$ is the estimated class and the $L(Z)$ is the likelihood function that we define and evaluate as:

(1) $L(Z) = p(Z_{e,X}, Z_{e,Ka}, Z_{e,W})$, the 3D joint-distribution function estimated from the data;

(2) $L(Z) = p_m(Z_{e,X}, Z_{e,Ka}, Z_{e,W})$, the 3D joint-distribution function modelled as a multivariate Gaussian distribution;

(3) $L(Z) = p(Z_{e,X})p(Z_{e,Ka})p(Z_{e,W})$, the independent 3D joint-distribution function.

All the supervised MLC are evaluated in terms of probability of detection (POD), false alarm rate (FAR) and the critical success index (CSI) are also shown.

3 Results

Four snowfall events during the BAECC campaign are used to investigate the impact of the rimed snow classification done in Falconi et al., 2018. In Figure 2 (a) the events were classified into three subgroups using a k-means cluster analysis trained by LWP and D_0. The riming is clearly related to LWP but almost not dependent on the estimated size.

We want now relate the classification made with the LWP evaluated by MWR to ground-based measurements estimated by PIP. For this purpose, a direct relation between the LWP and W, S is expected and visible in Figure 2(b), where W and S are conveniently scaled. In Figure 2(c) the k-means cluster analysis is reported on the W-S space in which the separation of the three-classes is visible and divided in three cones.

To relate the radar observables with the LWP classification three different supervised MLC have been applied. The four events are divided in a training dataset (12 February, 15/16 February and 22 February 2014) and a test dataset (21 February and 20 March 2014). In Table 1 the performance indexes are presented, showing the unlikelihood to classify the three classes. The MLC has been testes for a new classification model separating all the data in two classes: low riming (LOW = LR+MR) and heavy riming (HEAVY= HR) class. Looking at the results for two classes (Table 1), the possibility to classify is more concrete having a POD at around 0.75 for each class.

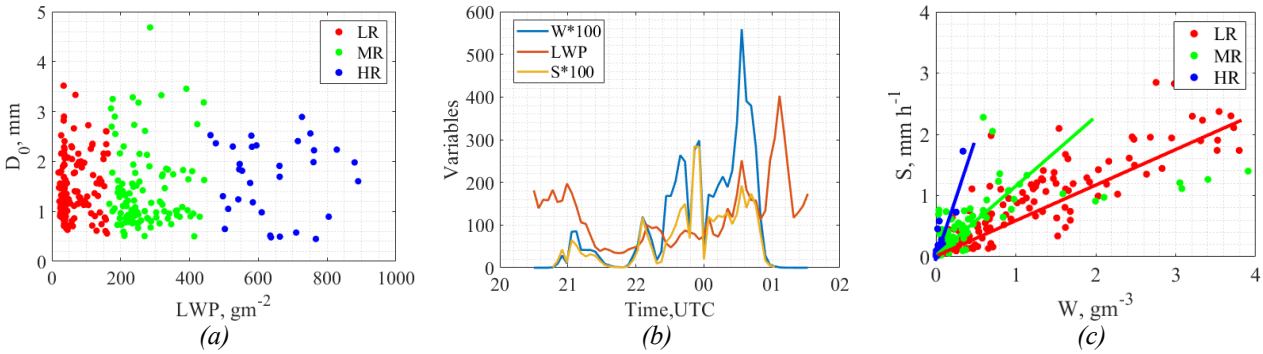

Figure 2: Comparison of ground-based evaluated variables and microwave radiometer measurements: (a) Plot of median diameter D_0 with respect to LWP for the three cluster regions: LR, MR and HR (red, green, blue) obtained on four snowfall days of BAECC IOP campaign; (b) Measurements from 15-16 February 2014 between 20:00 and 02:00 UTC, W and S are estimated by PIP and LWP is evaluated by MWR; (c) Three regions cluster in (b) are mapped into a S-W plane, defining three cones.

Table 1:Performance indexes for the three versions of the MLC.

	Two-classes			Three-classes		
L(z)	CSI	POD	FAR	CSI	POD	FAR
$p(Z_{e,X}, Z_{e,Ka}, Z_{e,W})$	0.68	0.75	0.25	0.13	0.23	0.77
$p_m(Z_{e,X}, Z_{e,Ka}, Z_{e,W})$	0.38	0.42	0.58	0.08	0.14	0.86
$p(Z_{e,X})p(Z_{e,Ka})p(Z_{e,W})$	0.69	0.73	0.27	0.23	0.38	0.62

References

von Lerber, A., Moisseev, D., Bliven, L. F., Petersen, W., Harri, A., and Chandrasekar, V.: Microphysical properties of snow and their link to Ze–S relations during BAECC 2014, J. Appl. Meteorol. Clim., 56, 1561–1582, https://doi.org/10.1175/JAMC-D-16- 0379.1, 2017.

Falconi, M. T., von Lerber, A., Ori, D., Marzano, F. S., and Moisseev, D.: Snowfall retrieval at X, Ka and W bands: consistency of backscattering and microphysical properties using BAECC ground-based measurements, Atmos. Meas. Tech., 11, 3059-3079, https://doi.org/10.5194/amt-11-3059-2018, 2018.

Sekelsky, S. M.: Near-field reflectivity and antenna boresight gain corrections for millimeter-wave atmospheric radars, J. Atmos. Ocean. Tech., 19, 468–477, https://doi.org/10.1175/1520- 0426(2002)0192.0.CO;2, 2002.